Controlling chaos in a weakly coupled array of Bose-Einstein condensates

Guishu Chong, Wenhua Hai,* and Qiongtao Xie
Department of Physics, Hunan Normal University, Changsha 410081, China
(Received 17 April 2004; published 3 January 2005)

The spatial structure of a Bose-Einstein condensate loaded into an optical lattice potential is investigated and the spatially chaotic distributions of the condensates are revealed under the tight-binding approximation. Adding a laser pulse on a proper site of the lattice and treating it as a control signal, control of the chaos in the system is carried out by using the Ott-Grebogi-Yorker scheme. For an appropriate laser pulse, we can suppress the chaos and push the system onto a stable manifold of a target orbit. After the control, a regular distribution, which may be expected in experiments or practical applications, of the condensates in the coordinate space is obtained.

DOI: 10.1103/PhysRevE.71.016202 PACS number(s): 05.45.Gg, 03.75.Lm, 05.30.Jp, 03.75.Kk

I. INTRODUCTION

Creation of the Bose-Einstein condensate (BEC) has provided a platform for investigating many important phenomena in atomic physics, condensed-matter physics, and quantum optics for the reason that this macroscopic quantum system consisting of ultracold atoms is unique in precision and flexibility for experimental control and manipulation [1–5]. The dynamics of the system is described by a Schrödinger equation combining with a nonlinear term, which represents the many-body interactions, in the mean-field approximation. This nonlinearity makes it possible to bring chaos into the quantum system. The existence of BEC chaos has been proved and the chaotic properties have also been extensively researched in many previous works [6–14]. Naturally, chaos, which plays a destructive role in the regularity of the system, will cause an instability of the condensate wave function [15]. The onset of the instability can lead to rapid proliferation of the thermal particles that has been observed experimentally [16]. Chaos in a collapsing BEC has also been discussed by Filho *et al.* [6] and Satio and Ueda [17]. Meanwhile, chaos is relevant to the phenomenon of macroscopic quantum self-trapping in BECs [12] and assists the instanton tunneling in the one-dimensional perturbed periodic potential [18]. Therefore, it is important to investigate the chaotic characteristics in the BEC system. For the purpose of applications control of chaos is anticipated in practical investigations.

Chaos control has always been a widely attractive field in recent decades since the pioneering work of Ott, Grebogi, and Yorker (OGY) in 1990 [19]. After the well-known OGY method, some methods such as the numerous simplifications, variations, and extensions have appeared and many efforts have been put into controlling chaos [20–24]. Overwhelmingly, these can be separated into two categories: feedback control (active control) and nonfeedback (passive) control. The general method for feedback control is to push a system state onto a stable manifold of a target orbit—that is to say, stabilizing the unstable target orbits embedded within a chaotic attractor.

In previous work we have investigated some chaotic characteristics in the BEC systems with a double-well potential [8,9] or a periodic one [10]. In the present paper, we consider a BEC array loaded into a periodically optical lattice potential. In the framework of the tight-binding approximation, we investigate the spatial structure of the condensates in the stationary state and find the chaotic features in the spatial distributions of the condensates. The presence of chaos will lead to a randomness in the spatial structure of the BEC and even a collapse of the matter wave. In order to control the chaos, we add a laser pulse, which can be expressed in the form of a δ-function potential and treated as a control signal, on an appropriate site of the optical lattice. Following the OGY method, if the control term is appropriate (with a certain strength or at a proper position) we can force the system to the stable manifold near an unstable periodic orbit. Consequently, a desired regular distribution of the BEC array can be achieved from the site where the control laser is added on.

This paper is organized as follows: spatially chaotic distributions of the stationary-state BECs are described in Sec. II. In Sec. III, the control of chaos is studied by using the OGY feedback control method. Finally, a summary is given in Sec. IV.

II. CHAOTIC DISTRIBUTIONS OF THE CONDENSATES IN OPTICAL LATTICES

For an ultracold vapor of bosonic atoms trapped in a magnetic well, pure condensates will be created when they are cooled to a temperature below the BEC threshold. After the creation, the BEC is loaded into a one-dimensional (1D) optical lattice potential which can be realized experimentally by a far-detuned, retroreflected laser beam [25,26]. The corresponding BEC dynamics is described by a time-dependent Gross-Pitaevskii equation (GPE) in the mean-field theory:

$$i\hbar\frac{\partial\Psi}{\partial t} = -\frac{\hbar^2}{2m}\nabla^2\Psi + [V_{ext} + V_L + g_0|\Psi|^2]\Psi, \qquad (1)$$

where m is the atomic mass and $g_0 = 4\pi\hbar^2 a/m$ denotes the atom-atom interaction with a being the s-wave scattering

*Corresponding author.
Electronic address: adcve@public.cs.hn.cn

length. The case $a>0$ represents a repulsive interatomic interaction, and $a<0$ implies the attractive case. The order parameter Ψ is normalized to the total number of the condensate atoms, N_T, $V_L=V_0\cos^2(kx)$ is the optical lattice potential, and V_{ext} denotes an external field superimposed on the lattice. When the heights of the interwell barriers of the optical lattice potential are much higher than the chemical potential of the system, the tight-binding approximation is a valid technique to account for the characters involved in the GPE [26–29].

In the framework of the tight-binding approximation, the optical lattices split the BEC into an array of many small BECs such that one can decompose the order parameter $\Psi(\vec{r},t)$ as a sum of wave functions localized in each well of the optical lattice potential:

$$\Psi(\vec{r},t)=\sqrt{N_T}\sum_n \psi_n(t)\Phi_n(\vec{r}), \tag{2}$$

where dimensionless function $\psi_n(t)$ is the nth amplitude and $\Phi_n(\vec{r})$ denotes the wave function localized in the nth lattice site, which weakly overlapped in the barrier region with the wave function $\Phi_{n\pm1}(\vec{r})$ in the neighbor sites. Inserting Eq. (2) into the GPE yields the discrete nonlinear Schrödinger equation (DNLSE) [26–29]

$$i\hbar\frac{\partial\psi_n}{\partial t}=-K(\psi_{n-1}+\psi_{n+1})+(\epsilon_n+U|\psi_n|^2)\psi_n. \tag{3}$$

Here [26], $K\simeq-\int d\vec{r}[(\hbar^2/2m)(\vec{\nabla}\Phi_n\cdot\vec{\nabla}\Phi_{n+1})+\Phi_n(V_{ext}+V_L)\Phi_{n+1}]$ is proportional to the microscopic tunneling rate between the adjacent sites and $U=g_0N_T\int d\vec{r}\Phi_n^4$ indicates the strength of the atom-atom interaction. In an experiment K is controlled by the strength of the optical potential and U is adjusted by using the technique of Feshbach resonance, respectively. Meanwhile, the energy functional given by $\epsilon_n=\int d\vec{r}[(\hbar^2/2m)(\vec{\nabla}\Phi_n)^2+(V_{ext}+V_L)\Phi_n^2]$ has a different form for different external fields V_{ext}. Note that the periodicity of the lattice leads the profile of Φ_n to the same one in any lattice site and, due to the tight binding, the Φ_n is localized in the nth well approximately. Therefore, the strength of the two-body interaction U is a constant which is independent of n. On the other hand, the tunneling rate K also was treated as a constant approximately in Ref. [26], because of the high localizations of the tight-binding states. However, the on-site energy ϵ_n should be a function of n, since V_{ext} depends on the spatial coordinates labeled by n and there is no overlap integral is involved in the expression of the on-site energy. For instance, it is proportional to n^2 for a harmonic confinement potential superimposed on the lattice potential in the experiment [26]. In Ref. [25], a coherent output of the matter waves was created by a vertical optical lattice which provides $\epsilon_n\propto n$ due to the gravity gradient.

In the present work, the external potential is taken as the form of a delta function $V_{ext}=\eta\delta(x-x_{n'})$ with η being the potential strength and $x_{n'}$ a fixed lattice site. As an "artificial" single impurity, such delta-function potential has been realized by a sharply focused laser beam in the experiment [30]. In this case, we obtain the integrations $\int d\vec{r}\Phi_nV_{ext}\Phi_{n+1}=0$ and $\int d\vec{r}V_{ext}\Phi_n^2=\eta\delta_{n,n'}$, because of the normalization condition $\int d\vec{r}\Phi_n\Phi_m\simeq\delta_{mn}$. So the tunneling rate K is indeed a constant for the periodic spatial distribution $\Phi_n(\vec{r})$ and the on-site energy ϵ_n consists of two terms: the $\eta\delta_{n,n'}$ and a constant. After absorbing the constant into the chemical potential (e.g., the latter E), the on-site energy reads [28,31] $\epsilon_n=\eta\delta_{n,n'}$ with $\eta>0(\eta<0)$ corresponding to the repulsive (attractive) cases and n' being the given lattice site on which the laser beam acts.

The DNLSE (3) has been studied extensively [26–29,32–37], although its dynamical behaviors are very complicated. For simplicity, we shall consider the case that the system is in the stationary state such that the amplitude ψ_n at the nth lattice site can be written as [33,38] $\psi_n=\chi_n\exp[-iEt/\hbar]$ with E being an arbitrary constant and χ_n a complex function of n. Substituting such ψ_n into Eq. (2), parentally, $\Psi(\vec{r},t)$ takes the form of the stationary solution, where E represents the chemical potential and χ_n is the dimensionless expansion coefficient associated with the basic vector $\Phi_n(\vec{r})$. For such time-periodic solutions the spatial properties of the system can be easily studied, because $|\chi_n|^2$ characterizes the fractional population N_n/N_T with N_n being the number of particles at the nth site. Employing the above form of ψ_n, Eq. (3) becomes

$$E\chi_n=-K(\chi_{n+1}+\chi_{n-1})+(\epsilon_n+U|\chi_n|^2)\chi_n \tag{4}$$

immediately. Rewriting the complex function in the exponential form $\chi_n=I_n\exp[i\theta_n]$ and inserting it into Eq. (4) we obtain the coupled equations for the fractional population amplitude I_n of the BEC at the nth site and the corresponding phase angle θ_n as

$$EI_n\cos\theta_n=-K(I_{n+1}\cos\theta_{n+1}+I_{n-1}\theta_{n-1})+(\epsilon_n+UI_n^2)I_n\cos\theta_n, \tag{5}$$

$$EI_n\sin\theta_n=-K(I_{n+1}\sin\theta_{n+1}+I_{n-1}\sin\theta_{n-1})+(\epsilon_n+UI_n^2)I_n\sin\theta_n. \tag{6}$$

After some simple calculations Eqs. (5) and (6) are changed to

$$I_{n+1}\cos(\Delta\theta_{n+1})+I_{n-1}\cos(\Delta\theta_n)=\frac{1}{K}(\epsilon_n+UI_n^2-E)I_n, \tag{7}$$

$$I_{n+1}\sin(\Delta\theta_{n+1})=I_{n-1}\sin(\Delta\theta_n), \tag{8}$$

with $\Delta\theta_n=\theta_n-\theta_{n-1}$. From Eq. (8) we observe that it defines a spatial evolution constant by

$$J\equiv I_nI_{n-1}\sin(\Delta\theta_n), \tag{9}$$

which is determined by the boundary values I_0, θ_0 and near boundary values I_1, θ_1 of the system. Following the studies in [39], introducing two newly dimensionless variables

$$w_n=I_n^2,\quad v_n=J\cot(\Delta\theta_n), \tag{10}$$

and combining Eqs. (7) with (9), we can yield a reduced two-dimensional map as

$$w_{n+1} = \frac{1}{w_n}(v_{n+1}^2 + J^2),$$

$$v_{n+1} = -v_n + \frac{1}{K}(\epsilon_n + Uw_n - E)w_n. \tag{11}$$

From the definitions of the new variables, we find w_n is just the fractional population at the nth site. When $\epsilon_n = 0$, the map (11) has been researched by Wan and Soukoulis [32] for the electronic response in a nonlinear lattice where the subindices n represent the time series contrasting with the spatial positions indicated here.

From the map (11) we can observe that when the interatomic interaction strength U is large enough the nonlinear effect will become dominant and the corresponding chaotic phenomenon will emerge. Consequently, the population of the BEC array becomes random in the spatial distribution. Furthermore, we can change the tunneling rate K by adjusting the height of the lattice and can control the two-body interaction intensity U by using Feshbach resonance in experiments. For certain boundary values of I_0, θ_0 and the near-boundary values I_1, θ_1, the spatial evolution constant J and the near-boundary values w_1, v_1 can also be determined as $J \equiv I_1 I_0 \sin(\theta_1 - \theta_0)$, $w_1 = I_1^2$, and $v_1 = J\cot(\theta_1 - \theta_0)$. Thus, given the tunneling rate K, nonlinear interaction strength U, chemical potential E, energy functional ϵ_n (which is determined by the externally added laser pulse and denotes the control signal in the next section), evolution constant J, and near-boundary values w_1, v_1, a series of BEC fractional populations w_n and v_n for $n = 2, 3, \ldots$ can be derived from Eq. (11). Consequently, the fractional populations of the BEC on every sites are acquired. According to these values of the fractional population w_n we can directly gain insight into the spatial structure of the condensates in the optical lattices. Many interesting properties of the electrons in the nonlinear lattice have been studied through the map (11) with $\epsilon_n = 0$ in Ref. [32]. Certainly, there have similar properties for the considered BEC system described by the map (11). Here, we shall pay attention to the chaotic features implied in this map, which is correlated to the spatially chaotic distributions of the BEC. The orbits generated by the mapping on the plane (w, v) can be either bounded or divergent for different parameter sets. The bounded orbits can further organize into a hierarchy orbits with different period due to the general theorem of Poincaré and Birkhoff and the KAM theorem [40]. Then, it is possible to find the chaotic trajectory near the hierarchy point [32].

Taking a set of system parameters as the tunneling rate $K = 0.5$, atom-atom interaction strength $U = 0.9$, chemical potential $E = 0.8$ [they are all in unit of atomic recoil energy $E_r = \hbar^2 k^2/(2m)$], and spatial evolution constant $J = 0.05$ associated with a certain boundary conditions and supposing the laser pulse is turn off (i.e., $\epsilon_n = 0$), we plot 20 orbits in the plane of dimensionless quantities (w, v) from mapping (11) with different initial iterations of $(w_1, v_1) = (0.1 + 0.005i, -0.1 + 0.005i)$, where i takes integer numbers from 1 to 20 and shown as in Fig. 1. In this figure, it is seen that around the fixed point there exist some invariant curves [32] and a

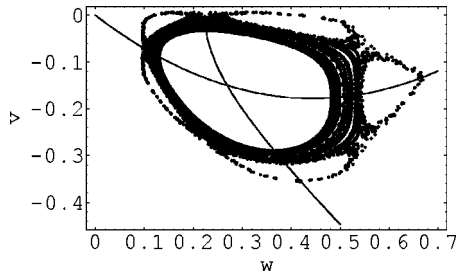

FIG. 1. Plot of the phase orbits with respect to dimensionless variables w, v. The dotted curves consisting of the 20 orbits for $(w_1, v_1) = (0.1 + 0.005i, -0.1 + 0.005i)$, $i = 1, 2, \ldots, 20$. The invariant curves, period-5 orbit, and the chaotic orbits surrounded them are illustrated. The two solid lines represent the symmetry lines from the equations $w = \sqrt{v^2 + J^2}$ and $v = Uw^2/2K - Ew/2K$, respectively, which give a fixed point as their cross point.

period-5 elliptic or hyperbolic orbit; the surrounding chaotic orbits are also demonstrated. When the interatomic interaction is attractive $(U < 0)$, a similar diagram for the orbits can also be achieved. Thereby, for certain system parameters and boundary conditions, the BEC system possesses a spatially chaotic distribution. This chaotic characteristic results in the stochasticity in the spatial structure of the BEC and destroys the regularity of the system. However, the stable periodic states are expected generally in experiments and practical applications. Due to the difficulty in precisely determining the boundary conditions of the BEC in experiments, we cannot acquire the desired periodic orbit through selecting the boundary conditions. So it is necessary to control the system from the chaotic state to the regular target state by using an effective control method. In the next section, we shall try to carry out this control.

III. CONTROLLING CHAOS IN THE SYSTEM

In the above discussion, the laser pulse has not been considered—i.e., $\epsilon_n = 0$. Obviously, in order to control the chaos, some control signal should be injected into the system. We shall take the laser pulse into account and find that it can be treated as the control signal for the BEC system. Using this externally imported field and selecting the unstable fixed point (period-1 orbit) of the mapping (11) as the target state, we shall control the chaos by stabilizing the system to the stable manifold of the objective state in the scheme of the OGY feedback control method. Following the OGY method [19,41] and starting from the mapping (11) with $w_{n+1} = w_n$ and $v_{n+1} = v_n$, we can obtain the fixed points governed by the coupled equations $w = \sqrt{v^2 + J^2}$ and $v = Uw^2/2K - Ew/2K$. After eliminating the coupling they read as

$$\alpha^2 w_F^4 - 2\alpha\beta w_F^3 + (\beta^2 - 1)w_F^2 + J^2 = 0,$$

$$\alpha(v_F^2 + J^2) - \beta\sqrt{v_F^2 + J^2} - v_F = 0, \tag{12}$$

with $\alpha = U/2K$ and $\beta = E/2K$. We suppose that one of the fixed points (w_F, v_F) is a saddle point, which is embedded within a chaotic state that the system lies in. Our task is to

stabilize the system to the stable manifold through the saddle point. Defining a transpose of $\mathbf{x}_n$ as $\mathbf{x}_n^T=[w_n\ v_n]$ and considering the dynamics nearby the point, we have [19,41]

$$\Delta\mathbf{x}_{n+1}=\mathbf{f}_\mathbf{x}\Delta\mathbf{x}_n,\quad \Delta\mathbf{x}_n=\mathbf{x}_n-\mathbf{x}_F, \tag{13}$$

with

$$\mathbf{x}_F=\begin{bmatrix} w_F \\ v_F \end{bmatrix}.$$

Here, $\mathbf{f}_\mathbf{x}$ is a 2×2 Jacobian matrix of the map (11), which determines the motive flow of the system at this fixed point and is given as

$$\mathbf{f}_\mathbf{x}=\left.\frac{\partial\mathbf{f}}{\partial\mathbf{x}_n}\right|_{\mathbf{x}_n=\mathbf{x}_F} =\begin{bmatrix} (\alpha w_F-\beta)(2\alpha w_F-\beta)+1 & -(\alpha w_F-\beta) \\ 2\alpha w_F-\beta & -1 \end{bmatrix}, \tag{14}$$

where $\mathbf{f}$ denotes the mapping. When the control signal is turned on, a shift to the unstable fixed point will be induced and is characterized by a linear response matrix as [41]

$$\mathbf{g}=(\mathbf{I}-\mathbf{f}_\mathbf{x})^{-1}\mathbf{f}_{\epsilon_n}|_{\mathbf{x}_n}=\mathbf{x}_F=\begin{bmatrix} 1/(2\alpha w_F-\beta) \\ 1 \end{bmatrix}, \tag{15}$$

with

$$\mathbf{f}_{\epsilon_n}=\left.\begin{bmatrix} \partial w_{n+1}/\partial\epsilon_n \\ \partial v_{n+1}/\partial\epsilon_n \end{bmatrix}\right|_{\epsilon_n=0}=\begin{bmatrix} 0 \\ 1/K \end{bmatrix}.$$

Since the fixed point $\mathbf{x}_F$ is a saddle point, the matrix $\mathbf{f}_\mathbf{x}$ should has the eigenvalues λ_u and λ_s. The former satisfies $|\lambda_u|>1$ and corresponds to motion along the unstable manifold. Contrarily, the latter obeys $|\lambda_s|<1$ and denotes motion along the stable manifold. From λ_s and λ_u, we can easily obtain the relevant stable and unstable eigenvectors $\mathbf{e}_s,\mathbf{e}_u$, respectively, by solving the eigenequations

$$\mathbf{f}_\mathbf{x}\mathbf{e}_u=\lambda_u\mathbf{e}_u,\quad \mathbf{f}_\mathbf{x}\mathbf{e}_s=\lambda_s\mathbf{e}_s. \tag{16}$$

The center manifold theory [42] correlates the stable manifold M_s and unstable manifold M_u to the stable and unstable eigenvectors $\mathbf{e}_s,\mathbf{e}_u$. Meanwhile, solving the equations

$$\mathbf{h}_u^T\mathbf{f}_\mathbf{x}=\lambda_u\mathbf{h}_u^T,\quad \mathbf{h}_s^T\mathbf{f}_\mathbf{x}=\lambda_s\mathbf{h}_s^T, \tag{17}$$

we can get the associated vectors $\mathbf{h}_u^T$ and $\mathbf{h}_s^T$, which satisfy the relations

$$\mathbf{h}_u^T\cdot\mathbf{e}_u=\mathbf{h}_s^T\cdot\mathbf{e}_s=1,$$

$$\mathbf{h}_u^T\cdot\mathbf{e}_s=\mathbf{h}_s^T\cdot\mathbf{e}_u=0, \tag{18}$$

and have the form of

$$\mathbf{h}_u^T=\left[\frac{-(\lambda_s+1)^{-1}}{[(\lambda_u+1)^{-1}-(\lambda_s+1)^{-1}]}\times\frac{1}{(2\alpha w_F-\beta)[(\lambda_u+1)^{-1}-(\lambda_s+1)^{-1}]}\right],$$

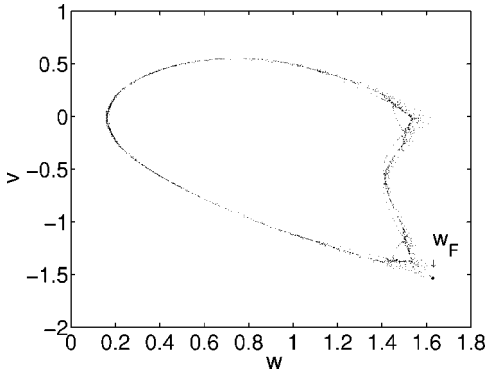

FIG. 2. Plot of the chaotic attractor from the map (11) in the plane of dimensionless quantities (w,v) with $\alpha=-0.524\,055$, $\beta=0.1$, and $J^2=0.25$. The target orbit of the unstable fixed point $(w_F,v_F)=(1.62,-1.53)$ is involved in it.

$$\mathbf{h}_s^T=\left[\frac{-(\lambda_u+1)^{-1}}{[(\lambda_s+1)^{-1}-(\lambda_u+1)^{-1}]}\times\frac{1}{(2\alpha w_F-\beta)[(\lambda_s+1)^{-1}-(\lambda_u+1)^{-1}]}\right]. \tag{19}$$

Supposing the spatial distributions of the condensates are chaotic when the control laser is turned off and the correspondingly chaotic attractor of the map (11) involves the unstable period-1 orbit. Meanwhile, on the (n')th site, if the fractional population $w_{n'}$ is very near to the fixed point, we add a weak laser pulse on this site, which means that the control signal is opened up. For the sake of controlling the chaos, the perturbation caused by the control laser should place the system state's next iteration $\mathbf{x}_{n'+1}$ in the stable manifold M_s of $\mathbf{x}_F$. This requires that $\Delta\mathbf{x}_{n'+1}$ have no component in the direction of the unstable manifold M_u which implies that $\Delta\mathbf{x}_{n'+1}\cdot\mathbf{h}_u^T=0$; therefore, the control rule for the OGY is given as [41]

$$\mathbf{h}_u^T\cdot\mathbf{x}_{n'+1}=\mathbf{h}_u^T\cdot\mathbf{g}\epsilon_{n'}+\lambda\mathbf{h}_u^T\cdot\Delta\mathbf{x}_n'-\lambda_u\mathbf{h}_u^T\cdot\mathbf{g}\epsilon_{n'}=0. \tag{20}$$

Applying $\epsilon_n=\eta\delta_{n,n'}$ to Eq. (20), the strength of the control signal is obtained as

$$\eta=\frac{\lambda_u\mathbf{h}_u^T\cdot\Delta\mathbf{x}_{n'}}{(\lambda_u-1)\{\mathbf{h}_u^T\cdot\mathbf{g}\}}. \tag{21}$$

In order to illustrate the processes of chaos control clearly, we shall set a group of system parameters and boundary conditions and give a numerical simulation. Setting the parameters as $\alpha=-0.524\,055$, $\beta=0.1$, and $J^2=0.25$, and the boundary conditions are given as $(w_1,v_1)=(0.5,0.5)$ we plot the orbit from mapping (11) in the plane of dimensionless quantities (w,v) which are shown as in Fig. 2. From Fig. 2 we find that the orbit is organized by a diffused point set but not a closed curve; the unstable fixed point (w_F,v_F) is embedded within the boundary of this chaotic attractor. Due to the properties that the chaotic orbit can come through all states in the chaotic attractor, this trajectory will reach the region which has arbitrarily small distance to the unstable

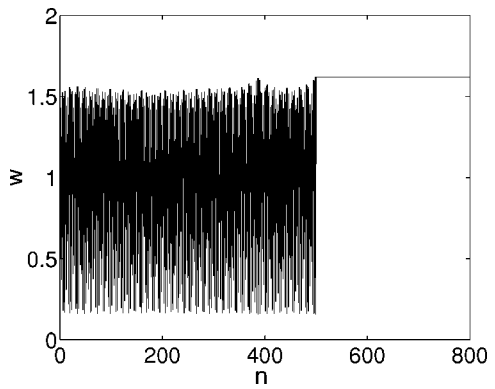

FIG. 3. Iterates of dimensionless quantities w_n from the map (11) controlled by the OGY method with $(w_1, v_1)=(0.5, 0.5)$. The system parameters are taken as $\alpha=-0.524$, $\beta=0.1$, and $J^2=0.25$.

orbit for many times in the moving procession. Thus this period-1 orbit can be selected as the target state.

Employing the same parameters in Fig. 2 and the above formula (12) we get the unstable fixed point $(w_F, v_F)=(1.62, -1.53)$. The corresponding matrixes in Eqs. (14) and (15) read

$$\mathbf{f_x}=\begin{bmatrix} 2.715 & 0.951 \\ -1.803 & -1 \end{bmatrix}, \quad \mathbf{g}=\begin{bmatrix} -0.5547 \\ 1 \end{bmatrix},$$

and the eigenvalues of $\mathbf{f_x}$ are easily produced as $\lambda_u=1.96$, $\lambda_s=-0.51$. Therefore, from Eqs. (16) and (19), the transpose of the eigenvectors and the associated orthogonal vectors are given as $\mathbf{e}_u^T=[1\ -0.9197]$, $\mathbf{e}_s^T=[1\ -3.67912]$ and $\mathbf{h}_u^T=[1.198\ 0.326]$, $\mathbf{h}_s^T=[-0.198\ -0.326]$, respectively. Eventually, according to the numerical result at the 498th iteration we have $\Delta\mathbf{x}_n^T=[-0.002, 0.025]$ with very small elements, which means the chaotic orbit is very near to the target state at this site. Hence, from the control rule of Eq. (21) the control parameter is calculated as $\eta=-0.035$. Injecting an attractively "artificial" impurity with above strength on the 498th iteration, we can push the system onto the stable manifold of the target state which is demonstrated in Fig. 3.

In Fig. 3 we show that the mapping evolves 498 iterations on a chaotic attractor before the control is activated. Then, the evolution of the map rapidly converges to the fixed point (w_F, v_F). Hence, the system has a chaotic distribution in the spatial positions from the first lattice site to the 498th site. After the 498th site, where the proper control is opened up, the distributions of the BECs are controlled to the stable manifold near the unstable periodic orbit and then to the fixed point associated with the target orbit rapidly. By the constant $w=w_F=1.62$ in Fig. 3 we mean that a fixed number of atoms is localized at individual lattice site after the 498th site. Note that for a trap of 1 mm size and laser wavelength of the order of 10^{-7} m, the number of optical lattice is about 10^4, which is much greater than 498. Particularly, we can set the control at the position that is much less than the 498th lattice coordinate. So, importing an appropriate sharply focused laser beam on the proper position of the lattice, one can change the spatial structure of the condensates from a chaotic distribution to a regular one for most of the lattice sites. The anticipatively regular BEC maybe has some practical applications.

In the above discussions, we mainly investigated the spatial properties of the BEC system. Of course, the time characters of the system are also attractive; for instance, the temporal stability of the target state is extremely important for applicable purposes. However, the target orbits contain some unstable periodic ones in general chaos control theories [19–21]. Due to the instability of the target orbit, the noises have significant effects on the control of chaos. In principle, we can adjust the control signal constantly to suppress the noise-induced derivation from the stabilized state, whereas, in order to strictly control the considered system both in time and space, we should control the spatiotemporal chaos as a whole. Generally, for the spatiotemporal system, its dynamical behaviors are described by the partial differential equations because it possesses both time and spatial variables. For such a partial differential equation system, both analytical treatments and numerical calculations are all the more complicated than the one-dimensional chaotic system. Considering the present BEC system and using a method being similar to that in [19], one can also form a $(m+1)$-dimensional delay-coordinate vector in the time series $\vec{X}(t)=(|\psi_n(t)|, |\psi_n(t-T)|, |\psi_n(t-2T)|, \ldots, |\psi_n(t-mT)|)$ with T being the time delay. Using the data of the probability density $|\psi_n(t)|^2$ we can construct a chaotic orbit in the $(m+1)$-dimensional reconstructed phase space. Generally, dimensions of the delay-coordinate vector can be chosen as the dimensions of the variables in practical system. Here, the two-dimensional delay-coordinate vector is considered for the reason that the one spatial coordinate and one time variable are involved in the system. Similar to Ref. [19], setting $|\psi_n(t-T)|=$const, one can obtain a series of cross points of the orbit $\vec{X}(t)$ with beeline $|\psi_n(t-T)|=$const. Denoting the coordinate of the ith cross point on the beeline by $\xi_n(i)$ and considering Eq. (3), one can get a map of the dynamical variable $\vec{X}(t)$ on the beeline. Therefore, after using the discrete time, the dynamics of the system can be described by the general form

$$\xi_n(i+1)=\mathcal{F}(\xi_{n+1}(i), \xi_n(i), \xi_{n-1}(i), p_n(i)), \tag{22}$$

where i and n are the time and space series, respectively, $\mathcal{F}$ denotes the map, and $p_n(i)$ represents the control signals.

Equation (22) describes the coupling map lattices (CML) model, which is the convenient spiflication of the real spatiotemporal systems [43]. When spatiotemporal chaos arises, rich motion states are involved in it. The target orbit with time periodicity and spatial uniformity discussed above is also governed by the CML model. For the CML model, different methods, such as the feedback pinning technique [20,44], delayed-feedback method [45], and decentralized delayed-feedback control approach [46], have been developed to control the spatiotemporal chaos and push the system to the state that is order in space and periodic in time. Therefore, similar control methods can be used for the present spatiotemporal chaotic system. A detail treatment for control

of spatiotemporal chaos will be given elsewhere, because of its importance and complexity.

IV. CONCLUSIONS

In summary, applying the tight-binding approximation we have investigated the spatial structure of a weakly coupled BEC array in an optical lattice. The chaotic features in the spatial distributions of the BEC for the stationary state were revealed. This kind of chaotic property maybe has a destructive role in the formation of the matter wave and is also not expected in the application of the BEC. So, injecting a control signal represented by a δ potential, which can be easily realized by a laser pulse in an experiment, we managed to control the chaos in the scheme of the well-known OGY feedback control method. The results showed that, adding the control signal with fit intensity on the apt site, the system can be pushed onto the stable manifold of the target orbit. This control enables us to obtain an expected distribution in the spatial positions from the site that the control laser is added on. Essentially, procession of controlling chaos is to obtain a regularly spatial BEC population, through the properly of a small modulation induced by an laser pulse to the structure of the optical lattice, rather than through an adjustment to the height or wavelength of the lattice. Suppression of chaos in the former case is valid and in the latter case is at the expense of the distinct change of the system which is considered generally as invalid in the theory of chaos control [41].

It is well known that the periodic lattice systems in BEC contain many fantastic properties. For example, quantum computation with BEC atoms in a Mott insulating state is an interesting advancement in applications of the BEC [47]. On the other hand, chaos is associated with quantum entanglement [48] and quantum error correcting [49] which are both the fundamental subjects in quantum computations. Thus, it is valuable to apply or control the chaos in the system.

ACKNOWLEDGMENT

This work was supported by the National Natural Science Foundation of China under Grant No. 10275023.

[1] F. Dalfovo, S. Giorgini, L. P. Pitaevskii, and S. Stringari, Rev. Mod. Phys. **71**, 463 (1999).
[2] S. L. Rolston and W. D. Phillips, Nature (London) **416**, 219 (2002).
[3] J. R. Anglin and W. Ketterle, Nature (London) **416**, 21 (2002).
[4] C. Orzel, A. K. Tuchman, M. L. Fenselau, M. Yasuda, and M. A. Kasevich, Science **291**, 2386 (2001).
[5] W. Ketterle, Rev. Mod. Phys. **74**, 1131 (2002).
[6] V. S. Filho, A. Gammal, T. Frederico, and L. Tomio, Phys. Rev. A **62**, 033605 (2000).
[7] H. R. Brand and R. J. Deissler, Phys. Rev. E **58**, R4064 (1998).
[8] W. Hai, C. Lee, G. Chong, and L. Shi, Phys. Rev. E **66**, 026202 (2002); Q. Xie, W. Hai, and G. Chong, Chaos **13**, 801 (2003).
[9] C. Lee, W. Hai, L. Shi, X. Zhu, and K. Gao, Phys. Rev. A **64**, 053604 (2001).
[10] G. Chong, W. Hai, and Q. Xie, Chaos **14**, 217 (2004); Phys. Rev. E **70**, 036213 (2004).
[11] Yu. Kagan, E. L. Surkov and G. V. Shlyapnikov, Phys. Rev. A **55**, R18 (1997).
[12] P. Coullet and N. Vandenberghe, Phys. Rev. E **64**, 025202 (2001).
[13] R. Franzosi and V. Penna, Phys. Rev. E **67**, 046227 (2003).
[14] Q. Thommen, J. C. Garreau, and V. Zehnlé, Phys. Rev. Lett. **91**, 210405 (2003).
[15] A. Vardi and J. R. Anglin, Phys. Rev. Lett. **86**, 568 (2001); G. P. Berman, A. Smerzi, and A. R. Bishop, *ibid.* **88**, 120402 (2002); C. Zhang, J. Liu, M. G. Raizen, and Q. Niu, *ibid.* **92**, 054101 (2004).
[16] Y. Castin and R. Dum, Phys. Rev. A **57**, 3008 (1998); Phys. Rev. Lett. **79**, 3553 (1997).
[17] H. Saito and M. Ueda, Phys. Rev. Lett. **86**, 1406 (2001).
[18] V. I. Kuvshinov, A. V. Kuzmin, and R. G. Shulyakovsky, Phys. Rev. E **67**, 015201 (2003).
[19] E. Ott, C. Grebogi, and J. A. Yorke, Phys. Rev. Lett. **64**, 1196 (1990).
[20] Hu Gang and He Kaifen, Phys. Rev. Lett. **71**, 3794 (1993); Hu Gang and Qu Zhilin, *ibid.* **72**, 68 (1994); J. Xiao, G. Hu, J. Yang, and J. Gao, *ibid.* **81**, 5552 (1998).
[21] J. Gong and P. Brumer, Phys. Rev. Lett. **88**, 203001 (2002).
[22] G. Kociuba and N. R. Heckenberg, Phys. Rev. E **68**, 066212 (2003).
[23] J. Starrett, Phys. Rev. E **67**, 056221 (2003).
[24] C. Wieland, Phys. Rev. E **66**, 016205 (2002).
[25] B. P. Anderson and M. A. Kasevich, Science **282**, 1686 (1998).
[26] S. Burger *et al.*, Phys. Rev. Lett. **86**, 4447 (2001); F. S. Cataliotti *et al.*, Science **293**, 843 (2001).
[27] A. Trombettoni and A. Smerzi, Phys. Rev. Lett. **86**, 2353 (2001).
[28] A. Trombettoni, A. Smerzi, and A. R. Bishop, Phys. Rev. Lett. **88**, 173902 (2002).
[29] A. Smerzi, A. Trombettoni, P. G. Kevrekidis, and A. R. Bishop, Phys. Rev. Lett. **89**, 170402 (2002).
[30] S. Burger *et al.*, Phys. Rev. Lett. **83**, 5198 (1999); J. Denschlag *et al.*, Science **287**, 97 (2000).
[31] D. J. Frantzeskakis, G. Theocharis, F. K. Diakonos, P. Schmelcher, and Y. S. Kivshar, Phys. Rev. A **66**, 053608 (2002).
[32] Y. Wan and C. M. Soukoulis, Phys. Rev. B **40**, 12264 (1989); Phys. Rev. A **41**, 800 (1990).
[33] R. Scharf and A. R. Bishop, Phys. Rev. A **43**, 6535 (1991).
[34] A. Polkovnikov, S. Sachdev, and S. M. Girvin, Phys. Rev. A **66**, 053607 (2002).
[35] V. M. Kenkre and G. P. Tsironis, Phys. Rev. B **35**, 1473 (1987); V. M. Kenkre, H.-L. Wu, and I. Howard, *ibid.* **51**, 15841 (1995).

[36] M. I. Salkola, A. R. Bishop, V. M. Kenkre, and S. Raghavan, Phys. Rev. B **52**, R3824 (1995).
[37] J. C. Eilbeck, A. C. Scott, and P. S. Lomdahl, Chem. Phys. Lett. **113**, 29 (1985); Physica D **16**, 318 (1985); Y. Zolotaryuk and J. C. Eilbeck, J. Phys.: Condens. Matter **10**, 4553 (1998).
[38] A. Lahiri, S. Panda, and T. K. Roy, Phys. Rev. E **66**, 056603 (2002).
[39] T. C. Bountis, C. R. Eminhizer, and R. H. G. Helleman, in *Long-Time Prediction in Dynamics*, edited by C. W. Horton, Jr., L. E. Reichl, and V. G. Szebehely (Wiley, New York, 1983).
[40] V. I. Arnold and A. Avez, *Ergodic Problems of Classical Mechanics* (Benjiamin, New York, 1968).
[41] G. Hu, J. Xiao, and Z. Zheng, *Chaos Control* (Shanghai Scientific and Technological Education, Shanghai, 2000).
[42] J. Carr, *Applications of Center Manifold Theory* (Springer-Verlag, New York, 1981).
[43] K. Kaneko, Chaos **2**, 279 (1992); *Theory and Applications of Coupled Map Lattices* (Wiley, Chichester, 1993).
[44] R. O. Grigoriev, M. C. Cross, and H. G. Schuster, Phys. Rev. Lett. **79**, 2795 (1997).
[45] P. Parmananda, M. Hildebrand, and M. Eiswirth, Phys. Rev. E **56**, 239 (1997).
[46] K. Konishi, M. Hirai, and H. Kokame, Phys. Rev. E **58**, 3055 (1998).
[47] J. K. Pachos and P. L. Knight, Phys. Rev. Lett. **91**, 107902 (2003).
[48] K. Furuya, M. C. Nemes, and G. Q. Pellegrino, Phys. Rev. Lett. **80**, 5524 (1998).
[49] P. H. Song and D. L. Shepelyansky, Phys. Rev. Lett. **86**, 2162 (2001).